Bulletin of the Seismological Society of America, Vol. 100, No. 5A, pp. 1940–1951, October 2010, doi: 10.1785/0120100017

Detection of Short Time Transients from Spectrograms Using Scan Statistics

by Steven R. Taylor, Stephen J. Arrowsmith, and Dale N. Anderson

Abstract We present a methodology for the detection of small, impulsive signal transients using time-frequency spectrograms closely related to the emerging field of scan statistics. In local monitoring situations, single-channel detection of small explosions can be difficult due to the complicated nature of the local noise field. Small, impulsive signals are manifest as vertical stripes on spectrograms and are enhanced on grayscale representations using vertical detection masks. Bitmap images are formed where pixels above a defined threshold are set to one. A short-duration large bandwidth signal will have a large number of illuminated bits in the column corresponding to its arrival time. We form the marginal distribution of bit counts as a function of time, n_i, by summing columnwise over frequency. For each time window we perform a hypothesis test, H_0: signal + noise, by defining a probability model expected when a signal is present. This model is Bernoulli for signal versus no signal with probability of signal $= \rho_1$. We assume that n_i follows the binomial distribution and compute a probability of detection (represented as a p value) for a given ρ_1. We apply the spectrogram detector to 1 hr of single-channel acoustic data containing a signal from a 1 lb chemical surface explosion recorded at 3.1 km distance and compare performance with a short-term average to long-term average (STA/LTA) detector. Both detectors are optimized through grid search and successfully detect the acoustic arrival from the 1 lb explosion. However, 70% more false detections are observed for STA/LTA than for the spectrogram detector. At great range, attenuation properties of the earth reduce the effectiveness of the spectrogram detector relative to STA/LTA. Data fusion techniques using multiple channels from a network are shown to reduce the number of false detections.

Introduction

Time-frequency spectrograms have been the focus of many applications in seismology and infrasound. Relevant to explosion-source monitoring, time-frequency patterns manifest in ripple-fire mining explosions have been used to discriminate them from earthquakes (Hedlin *et al.*, 1989; Hedlin *et al.*, 1990) or single-charge explosions (Arrowsmith *et al.*, 2006). They have also been combined with artificial neural networks for signal detection (e.g., Wang and Teng, 1995). Most infrasound detection research has been applied to array detection (e.g., Brown *et al.*, 2008, who used Hough transforms) or multiple array detection (e.g., Arrowsmith *et al.*, 2008).

In this paper, we examine the utility of spectrograms for the single-channel detection of low-amplitude, short time transients having a large bandwidth (e.g., small explosions at local distances). In theory, detection of impulsive signals should be a trivial problem because of their short-duration and large bandwidth. In reality, the problem can be more complex because of complications due to extraneous time-varying noise sources, particularly in local monitoring situations. A spectrogram detector can be used as a reconnaissance tool for coarse examination of broadband short-signal transients. Once a detection is made, other higher resolution detectors can be used that are tuned to the signal of interest for either signal classification or onset time estimation. We follow a procedure closely related to the recently evolving field of scan statistics. Scan statistics are used in detecting temporal and spatial clusters for applications in disease surveillance, medical imaging, environmental monitoring, wireless sensor networks, and, importantly, the analogy of tracking of a Zamboni on a hockey rink (e.g., Naiman and Priebe, 2001; Guerriero *et al.*, 2008; Niu and Varshney, 2009; Guerriero *et al.*, 2009). Taylor (2009) applied a similar technique to explosion and earthquake discrimination problems using two-dimensional (2D) grids of P/S amplitude ratios of Fisk *et al.* (2009). We apply the technique to 1 hr of single-channel acoustic data containing a small signal from a 1 lb surface explosion recorded at a

distance of 3.1 km and compare results with a standard STA/LTA detector.

Although our application for development of the spectrogram detector is for the detection of small local explosions, the theory could be used at greater ranges and other source types. For example, we will show it can be applied to detection of small *P* waves at teleseismic distances. We will also apply the spectrogram detector to four stations recording teleseismic *P* waves from a nuclear explosion to illustrate how a network of detectors can be statistically combined. Other applications can include detection of footsteps, gunshots, acoustic signals from volcanoes (e.g., explosions and tremor) among others.

Spectrogram Detection

We wish to develop a detector specifically designed for short time transients using as much of the signal and signal spectrum as possible, thereby maximizing the detection time-bandwidth product. The problem is illustrated by the local seismic recording of a small explosion shown in Figure 1. The seismogram for the explosion (detonated at zero time) is shown in Figure 1b; the associated spectrogram is shown in 1a. The explosion manifests as a narrow broadband vertical spectral line located at zero time. Other signal transients observed at approximately +360 s are of longer duration and narrower bandwidth than the small explosion. Interestingly, a Doppler shift associated with a helicopter is observed initiating with the +360 s signals. There are also numerous continuous noise sources observed on the spectrogram as horizontal lines, presumably from local anthropogenic sources such as generators, cooling fans, and 60 Hz noise. In this case, the explosion could be easily detected using standard techniques such as STA/LTA. However, we use small explosions recorded on single-channel acoustic data to demonstrate that the spectrogram detector is superior to STA/LTA because it produces fewer false detections.

As will be discussed in detail later in this paper, the processing consists of the following steps

1. Compute grayscale spectrogram (f = frequency; t = time; Fig. 2a).
2. Run a 2D spatial filter over the spectrogram that emphasizes vertical stripes (called masks in image processing; Fig. 2b).
3. Set a threshold, β_1, based on a histogram of grayscale values and convert to a binary spectrogram (Fig. 2c).
4. Sum the columns and plot sum versus time for each time segment (Fig. 3).
5. Compute detection threshold at assigned significance level and flag detections (Fig. 3; dashed line).

For Step 1, we compute a grayscale (also known as monochrome or intensity) spectrogram using the moving window technique (Dziewonski *et al.*, 1969; Oppenheim and Schafer, 1989; Fig. 2a). By grayscale, we mean that the modulus (intensity) of the spectrogram is normalized

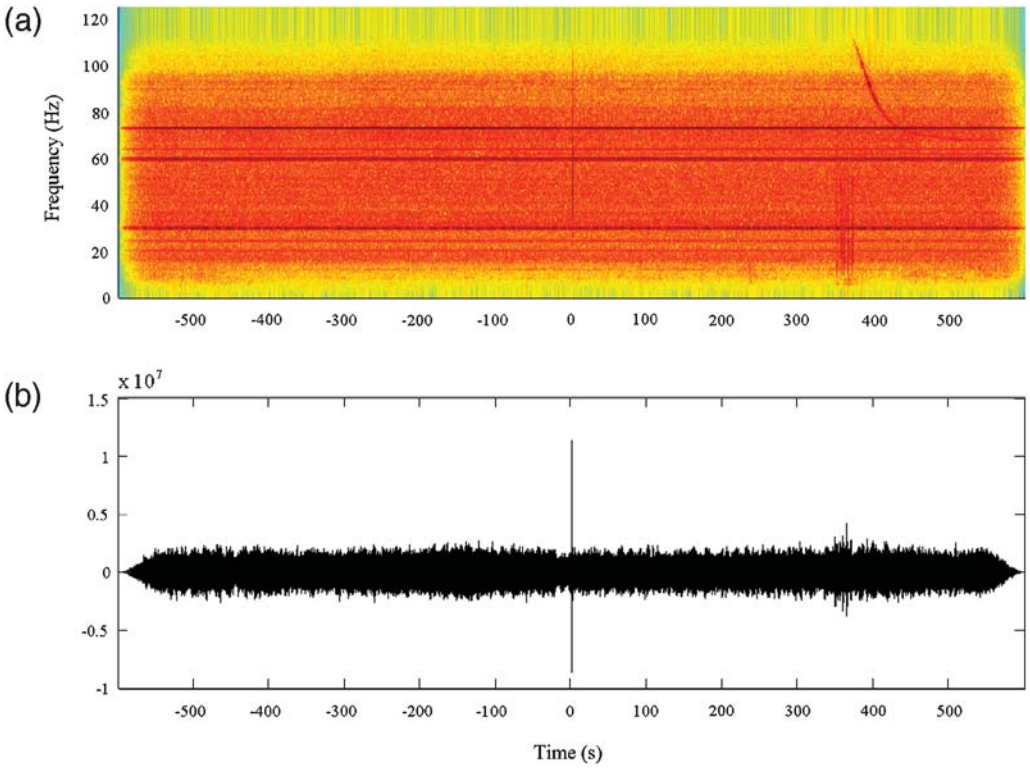

Figure 1. (a) Spectrogram and (b) seismogram for a small explosion detonated at zero time. Seismogram units are in counts proportional to ground velocity.

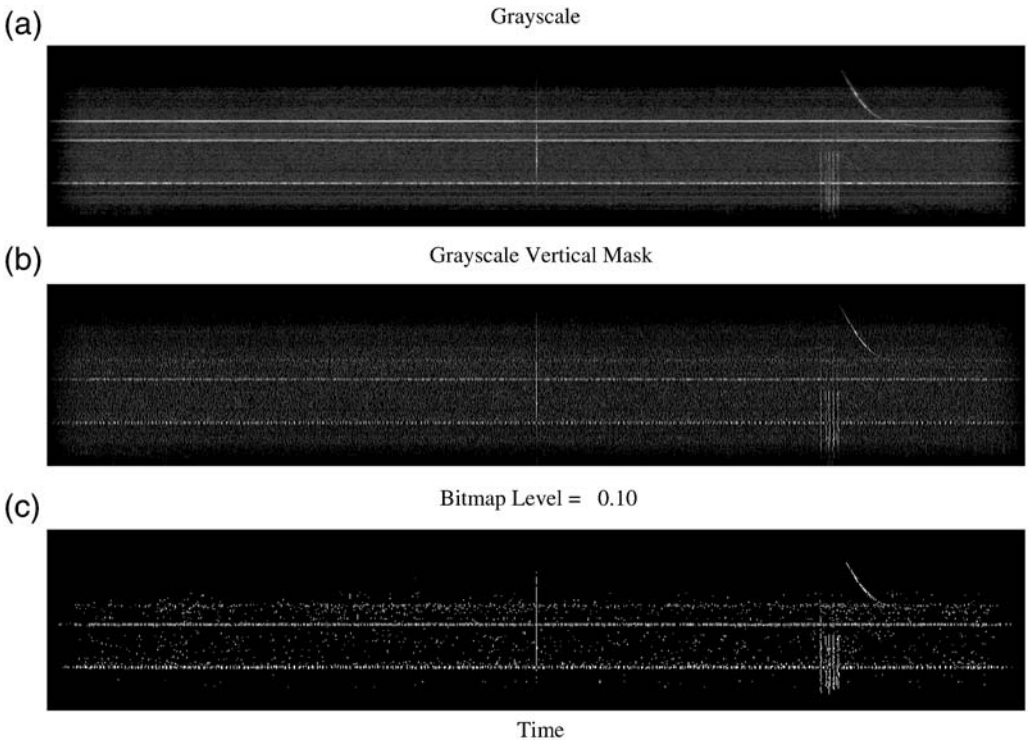

Figure 2. (a) Grayscale map of spectrogram shown in Figure 1. (b) Grayscale map after application of simple vertical mask. (c) Bitmap of middle plot using a normalized grayscale threshold of $\beta_1 = 0.1$.

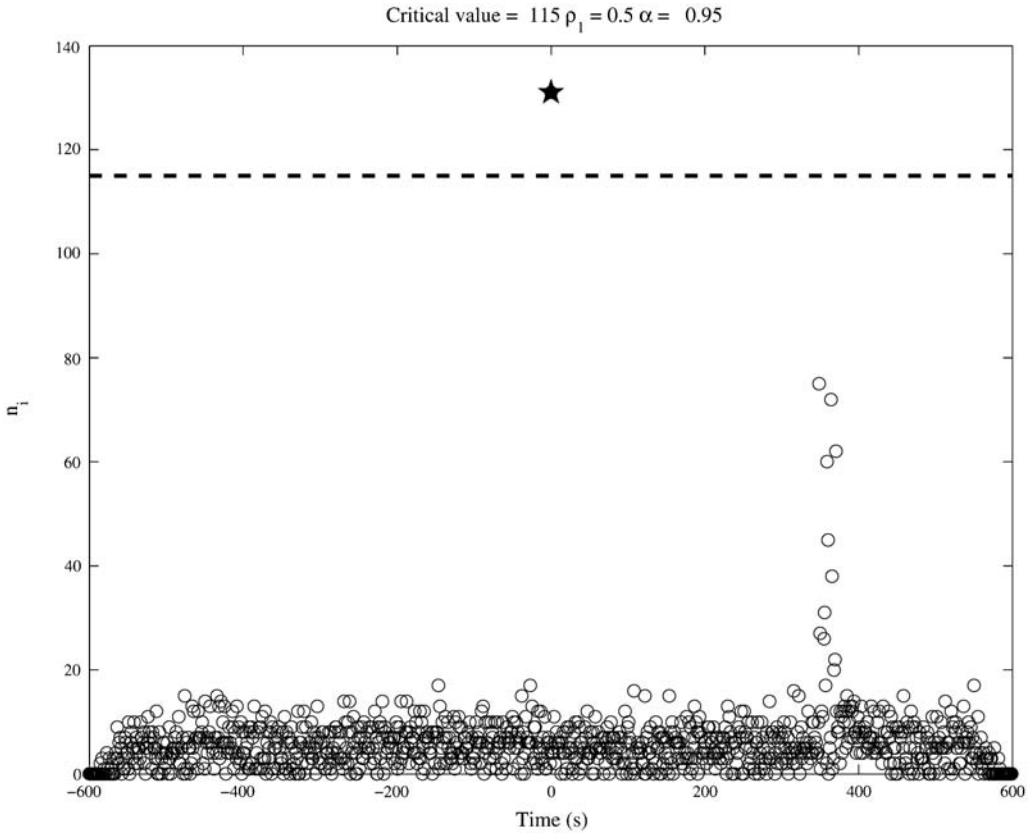

Figure 3. Number of ones, n_i, for each window t_i given by equation (3). Dashed line is the critical number of bits for a detection at a significance level of $\alpha = 0.95$ and $\rho_1 = 0.5$. Star indicates detection under H_0: signal + noise computed from equation (13).

to consist of values between 0 and 1. The time window length should be approximately that of the expected length of the signal transients to be detected. We then apply (Step 2) a 2D linear spatial filter designed to enhance vertical lines (e.g., Gonzalez and Woods, 2002; Gonzalez *et al.*, 2004; Fig. 2b). For illustration purposes, we use a simple linear 3 × 3 moving average filter with the coefficients

$$\begin{bmatrix} -1 & 2 & -1 \\ -1 & 2 & -1 \\ -1 & 2 & -1 \end{bmatrix}, \tag{1}$$

while noting that a number of other filters can be designed to enhance the desired spectral line. Equation (1) is basically a vertically orientated high-pass filter. As we will discuss later in this paper, different masks can be used depending on the signal characteristics. From Figure 2b, we see that the filter has the intended effect because the vertical spectral line associated with the small explosion is enhanced relative to the background. Finally (Step 3), the grayscale image is converted to a bitmap image, $b(t_i, f_j)$, consisting of only ones (white) and zeros (black) (Fig. 2c). This step of the processing involves the selection of a threshold value, β_1, above which the grayscale value becomes a one and below which the grayscale value becomes a zero so that

$$b(t_i, f_j) = \begin{Bmatrix} 1 & \text{if grayscale value} > \beta_1 \\ 0 & \text{otherwise} \end{Bmatrix}. \tag{2}$$

Note that β_1 is between 0 and 1 and can be selected from visual examination of a histogram of normalized intensity values. Otsu's method (Otsu, 1979) can be used that chooses a level based on the interclass variance between black and white pixels. In practice, we select β_1 based on a grid search of detection parameters over a set of training data. For the case of noise only, the ones will be randomly distributed. In contrast, a short-duration small (large bandwidth) explosion will have a large number of illuminated bits in the column corresponding to its arrival time. Use of the vertical detection mask helps remove some of the unwanted noise that can complicate the selection of β_1. We then form the marginal distribution of bit counts as a function of time by simply summing columnwise over frequency using

$$n_i = \sum_{j=1}^{n_f} b(t_i, f_j), \tag{3}$$

where n_f is the number of frequencies in the spectrogram and n_i is the number of frequencies having illuminated bits for each time window, t_i. Figure 3 shows the value of n_i for each time window of the binary spectrogram of Figure 2c.

The next step involves developing a statistical basis for declaring a detection. The technique that we have developed is very similar to that used in the recently evolving field of scan statistics described in the Introduction.

Statistical signal detection theory typically constructs a hypothesis test of the form

$$H_0\text{: } s(t) = \text{noise} \tag{4}$$

versus

$$H_A\text{: } s(t) = \text{signal + noise} \tag{5}$$

(e.g., Kay, 1998; Shumway and Stoffer, 2000). The Neyman–Pearson theorem states that the probability of detection will be maximized at a given acceptable false alarm rate, α, by deciding H_A if a likelihood ratio of the form exceeds a threshold λ

$$L(\mathbf{x}) = \frac{p(\mathbf{x}|H_A)}{p(\mathbf{x}|H_0)} > \lambda, \tag{6}$$

where p is a conditional probability density, $\mathbf{x}$ is a feature vector of measurements (discriminants), and α is given by

$$\alpha = 1 - \int_{-\infty}^{\lambda} p(\mathbf{x}|H_0) d\mathbf{x}. \tag{7}$$

In order for the likelihood ratio in equation (6) to be computed, the probability distribution of the noise as well as the signal must be known and can frequently be done using closed-form mathematical solutions. However, from the spectrogram shown in Figure 1, it can be seen that the noise characteristics can often be difficult to determine.

Our approach is to form the general null hypothesis

$$H_0\text{: signal + noise,} \tag{8}$$

and to construct a p value indicating the probability of detection conditional on the observations (e.g., Naiman and Priebe, 2001; Anderson *et al.*, 2007). The p value for the detected signal can also be thought of as indicating the typicality index (or degree of membership; McLachlan, 1992) that the signal originated from a small explosion. We chose the p-value formulation to conform to the newly proposed event identification framework of Anderson *et al.* (2007). In the p-value formulation, a physically based probability model is formulated for each discriminant under the general null hypothesis of the signature having characteristics of a small explosion. The p values range from zero to one where a moderate to large value indicates consistency with a small explosion and near zero otherwise. The p values from different detectors can be thought of as random variables and formed into standardized discriminants having approximately multivariate normal distributions. Well-established discrimination methods can be used to aggregate the transformed discriminants in order to form a multivariate probability of detection (e.g., Friedman, 1989; Anderson and Taylor, 2002). No assumptions are necessary for the signal from the alternative sources. In the following paragraphs, we will also discuss a procedure for combining p values from a small network of stations

From equation (3) we assume that n_i follows the binomial distribution

$$f_B(n_i|n_f,\rho_1) = \binom{n_f}{n_i}\rho_1^{n_i}(1-\rho_1)^{n_f-n_i}, \quad (9)$$

where $E[n_i] = n_f\rho_1$ and $\mathrm{var}[n_i] = n_f\rho_1(1-\rho_1)$. ρ_1 is the probability of success in a Bernoulli trial.

A binary spectrogram of pure random noise will be simply characterized by a probability density of ones given by

$$\rho_1^{\mathrm{noise}} = \frac{\sum_{i=1}^{n_t}\sum_{j=1}^{n_f} b(t_i,f_j)}{n_t n_f}, \quad (10)$$

where the product of n_t and n_f is the total number of points in the spectrogram. As can be seen from Figure 2c, the density will typically be very small except in the presence of a short-duration, broadband signal. Originally, we were going to construct a null hypothesis that we were observing noise; failure to accept the null would indicate the presence of a signal. However, because of the correlated noise sources often observed in local monitoring situations (as shown in Fig. 1), we decided to use the null hypothesis for the expected characteristics of an explosion. Our approach is to establish a value of ρ_1^{signal} for the signals of interest where

$$\rho_1^{\mathrm{signal}} = \frac{1}{n_f}\sum_{j=1}^{n_f} b(t_s,f_j), \quad (11)$$

and the summation is taken over the signal time window, t_s. For simplicity of notation we will substitute ρ_1 for ρ_1^{signal} in portions of the subsequent discussion. ρ_1^{signal} can be thought of as the probability of success in a signal window, assuming that n_i is a Bernoulli random variable.

To construct the null hypothesis of the form H_0: signal + noise, we define the p value indicating the probability of detection computed from the binomial cumulative distribution function (CDF) as

$$p_d = F_B(n_i|n_f,\rho_1) = \sum_{i=0}^{n_i}\binom{n_f}{i}\rho_1^{i}(1-\rho_1)^{n_f-i}, \quad (12)$$

which is the probability of observing up to n_i bits in n_f independent trials; the definition of ρ_1 is given by equation (11).

To find the number of counts above which to declare a detection, n_d, we first assign a critical value to the test, α, where $1-\alpha$ is the false alarm rate. The detection threshold (number of ones in a given time window) is computed from the inverse binomial CDF given α and ρ_1 using

$$n_d = F_B^{-1}(1-\alpha) = \sum_{n_i=0}^{\lfloor\alpha\cdot n_f\rfloor} f_B(n_i), \quad (13)$$

where $\lfloor x\rfloor$ is the floor of x given by the nearest integer less than or equal to x. Figure 4 shows the binomial PDF and CDF from which n_d is computed and shown as the solid line. In practice, a training set of calibration data is acquired, and a grid search is performed over various detection patterns using some criteria for acceptable error rates.

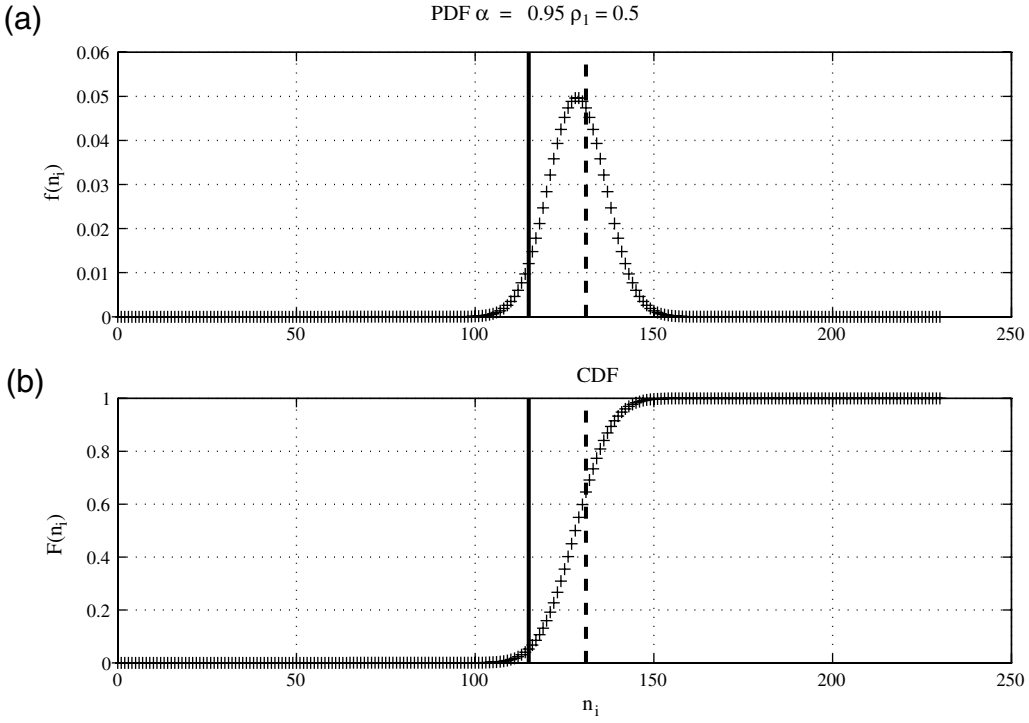

Figure 4. (a) Binomial PDF for $\alpha = 0.95$ and $\rho_1 = 0.5$ and (b) CDF bottom. Critical value of 115 (out of 257 frequency bins) shown as solid line is computed from the CDF (see dashed line in Fig. 3). Dashed line shows n_i (number of illuminated bits) for example in Figure 3 and corresponding p-value computation from cumulative distribution function whose value is indicated by star in Figure 5.

We would like to have the ability to construct p values for a number of detectors and combine them in a multivariate setting following Anderson *et al.* (2007), all under the null hypothesis H_0: signal + noise. For the null hypothesis we have chosen the p values for signal detections that will, in general, be uniformly distributed between 0 and 1 by the probability integral theorem (Rohatgi, 1976). In contrast, spectrogram bins having few illuminated bits will have small p values, as can be seen from Figure 4b. The probability of detection for the event in question is shown in Figure 5.

Next, we applied the spectrogram detector and a short-term average to long-term average (STA/LTA; Allen, 1982) detector to some of the small-explosion acoustic signals discussed in Arrowsmith (2009). We analyze a 1 hr time segment about a 1 lb surface detonation recorded at a single-channel acoustic station at 3.1 km. The window also includes a 400 lb surface explosion located at 5.4 km from the recording site. Figure 6 shows both explosions filtered between 1 and 40 Hz. Single-channel acoustic signals are often contaminated by noise bursts due to wind gusts and turbulence, which is why acoustic arrays are preferred but not always possible to deploy.

We optimized the spectrogram detector to the 1 lb signal by conducting a grid search over a large number of spectrogram detection parameters including different detection masks. The set of parameters was chosen that detected the target signal and minimized the number of false detections over the 1 hr time window. Overlapping Hanning time windows of length of 0.25 s were used with 256 fast Fourier transform frequency samples. Parameters of $\alpha = 0.9$, $\rho_1 = 0.4$, and $\beta_1 = 0.01$ along the vertical detection mask given by equation (1) gave the best results. There were a total of 12 single-channel false detections out of 5624 time segments in the 1 hr time window. Both the 1 lb and 400 lb explosions were detected. The results are shown in Figure 7 where the detections are indicated in red. Figure 8 is a magnification of Figure 7 for a 1 min time window around the 1 lb explosion.

Using the same 1 hr single-channel acoustic time series at station LTT03, we compare the spectrogram detector with the standard short-term average over long-term average (STA/LTA) detector (Allen 1982; Withers *et al.*, 1998) for the purposes of detecting locally recorded small explosions. The STA/LTA detector is simply a ratio of the mean square value of the signal in a short time window divided by a long time window. The mean square value of the short time window is given by

$$X_s^2 = \frac{1}{n_s}\sum_{i=1}^{n_s} s_i^2(t), \tag{14}$$

where $s(t)$ is the time series and n_s is the number of points in the short time window (i.e., the product of the short time window length in seconds and the sampling rate in Hz).

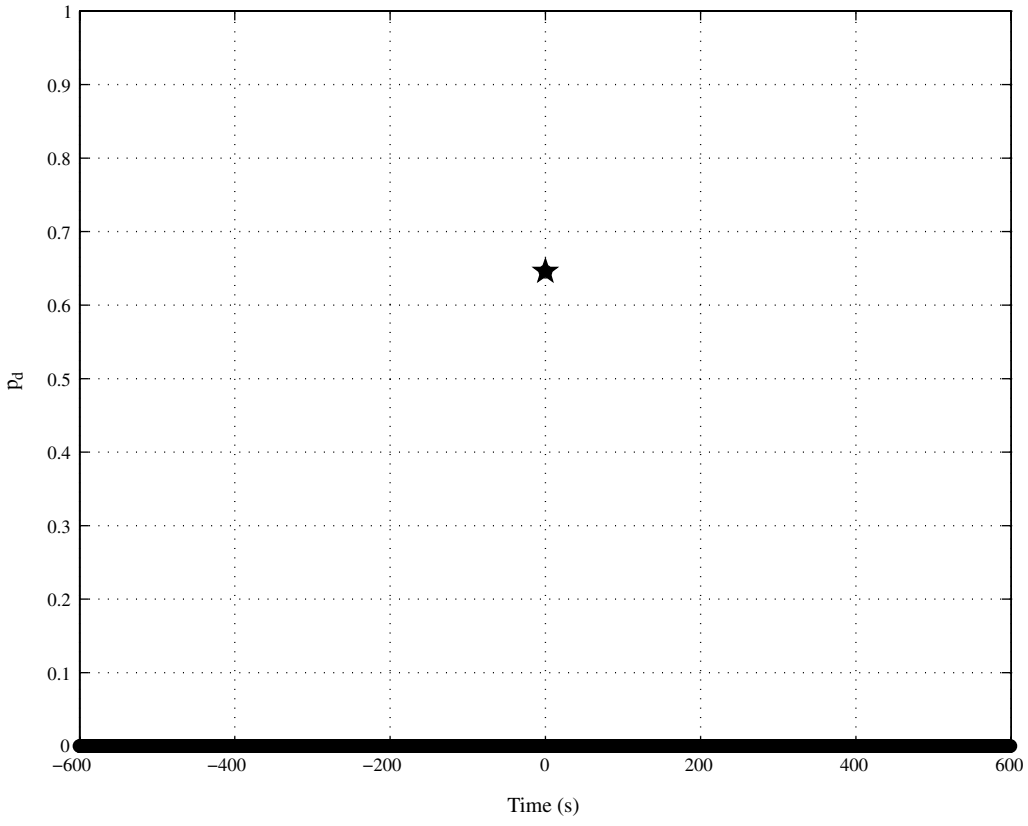

Figure 5. Probability of detection, p_d, for time series shown in Figure 1.

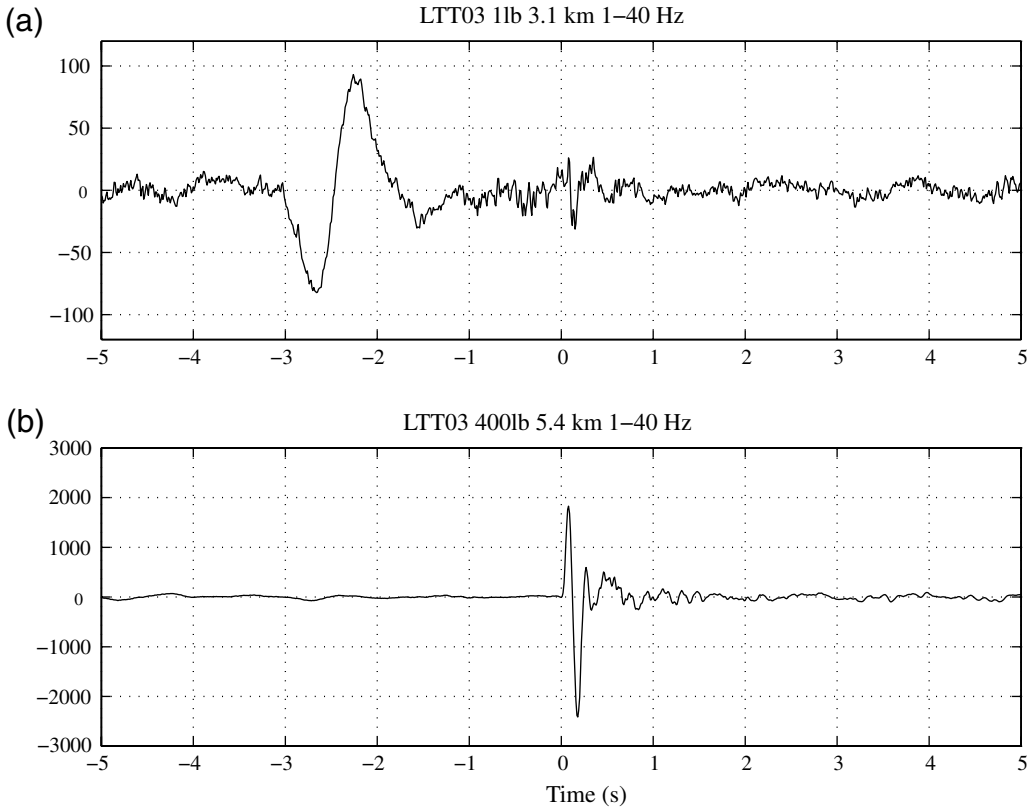

Figure 6. (a) Acoustic signals at station LTT03 for a 1 lb explosion and (b) 400 lb explosion conducted at Los Alamos National Laboratory. Arrivals for both explosions are centered at 0 s. Units are in counts proportional to pressure.

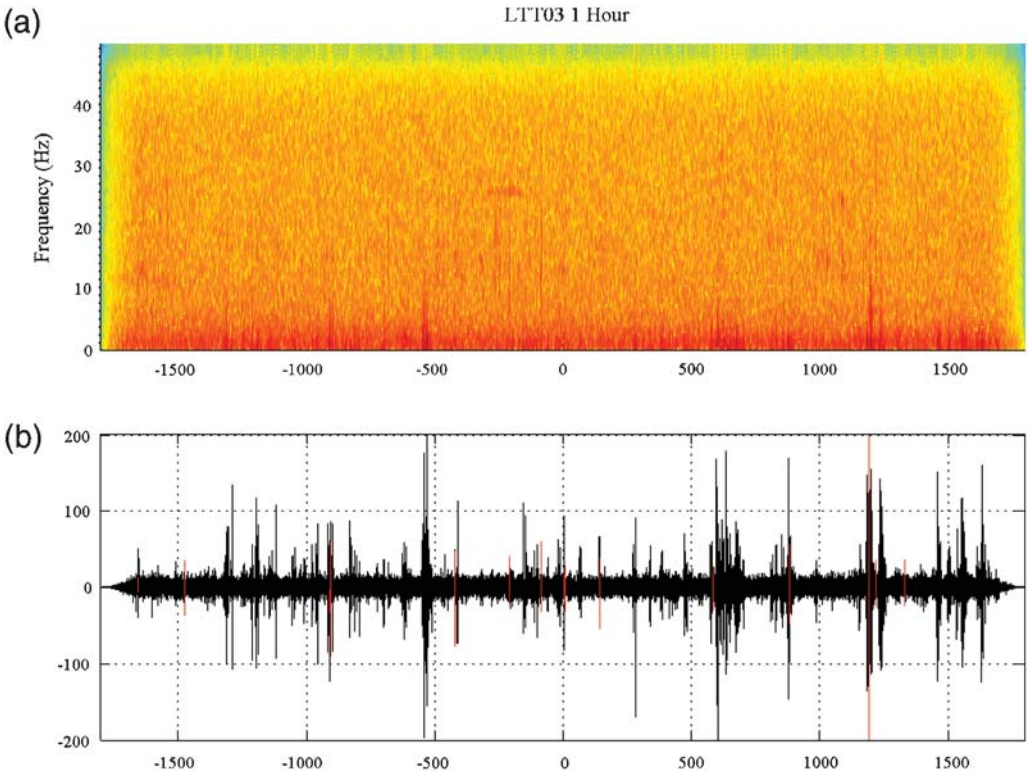

Figure 7. (a) Spectrogram for acoustic signals at station LTT03 for a 1 hr time segment centered on the 1 lb explosion shown in Figure 6a. (b) The amplitude of 400 lb explosion (Fig. 6b) is truncated in the lower portion and arrives at approximately 1200 s after the 1 lb explosion. Red segments indicate spectrogram detections (see text for details). Units of time series are in counts proportional to pressure.

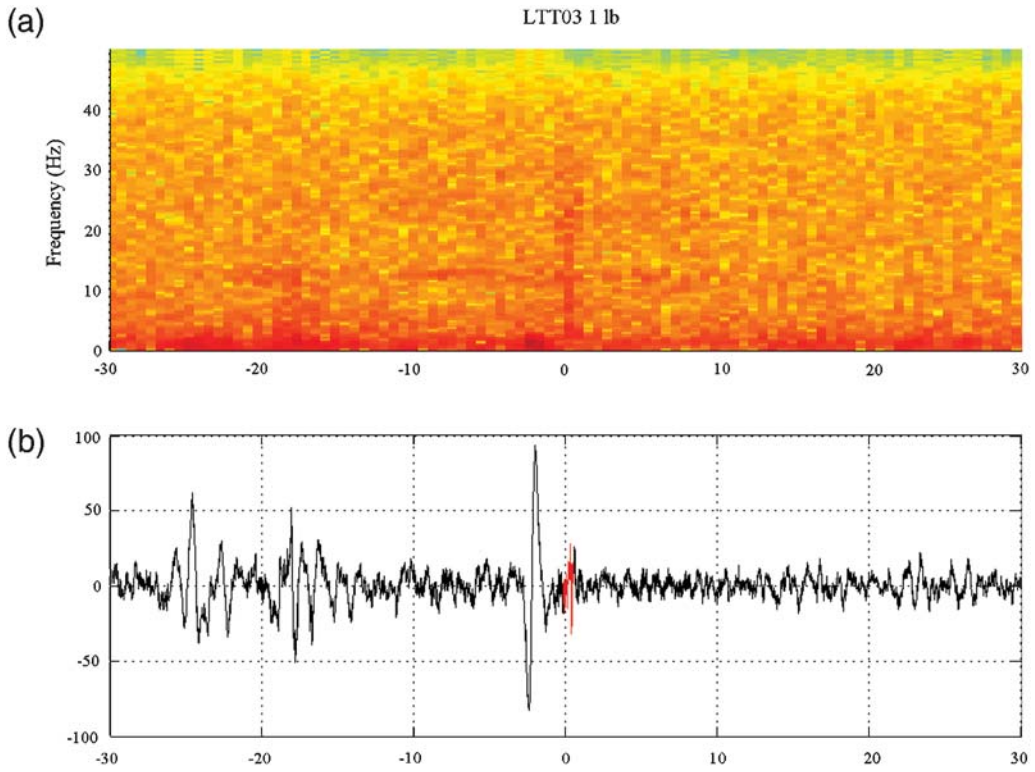

Figure 8. Same as Figure 7 but for a 1 min time segment around the arrival from the 1 lb explosion. Units of time series are in counts proportional to pressure.

Similarly, the mean square value of the long time window is given by

$$X_l^2 = \frac{1}{n_l}\sum_{i=1}^{n_l} s_i^2(t), \tag{15}$$

where n_l is the number of points in the long time window. In our analysis, the short-term window always leads the long-term window, and the two windows do not overlap in an effort to ensure statistical independence between the two values. The STA/LTA is then given by

$$\text{STA/LTA} = \frac{X_s^2}{X_l^2}. \tag{16}$$

We assume that for a single-channel, the STA/LTA follows a noncentral F for H_0: signal + noise (Blandford, 1974). In this case, no assumptions regarding the noise power spectrum are made, and for the null hypothesis of signal + noise the distribution for the STA/LTA is given by the noncentral F

$$\frac{X_s^2}{X_l^2} \sim F(N_s, N_l, \lambda), \tag{17}$$

where $N_s = 2T_sB$ is the degrees of freedom for the numerator, $N_l = 2T_lB$ is the degrees of freedom for the denominator, T_l is the length of the long-term window, B is the bandwidth, and $\lambda = N_s(S/N)^2$ is the noncentrality parameter where S/N is the signal-to-noise ratio. We construct a p value representing the conditional probability that an event is detected given that H_0 is true. In other words, we construct our statistical test so that if a p value is greater than a given significance level, we cannot reject the null hypothesis given by equation (8). Mathematically, we define the p value as

$$p = P(H_0|\text{STA/LTA}) = P\{F(N_s, N_l, \lambda) \geq F_\alpha\}, \tag{18}$$

where F_a is the critical value given by the inverse of the noncentral cumulative F distribution at a significance level α.

We performed a grid search over a wide range of detection parameters and selected the parameters that detected the 1 lb explosion and had a minimum number of false detections. It appears that a good frequency band to use in this case is 5 to 10 Hz with a short time window of 0.1 s, a long time window of 4 s, $\alpha = 0.99$, and noncentrality parameter of 2. The results are shown in Figure 9, where it can be seen there are 70% more false detections (20) than for the case of the spectrogram detector (12). The reason is that the acoustic signals show a number of short-duration high amplitude signals that trigger the STA/LTA detector. In contrast, the spectrogram detector does not trigger on many of these signals because of their limited bandwidth. We also ran the STA/LTA on a number of windows that included lower frequencies, just higher frequencies, or the same 1–40 Hz band used for the spectrogram detector; in all cases, many more false detections occurred.

The power of the spectrogram detector results from its ability to effectively exploit the broadband nature of the impulsive source. Therefore, its effectiveness is expected to decrease as propagation distance increases from the source.

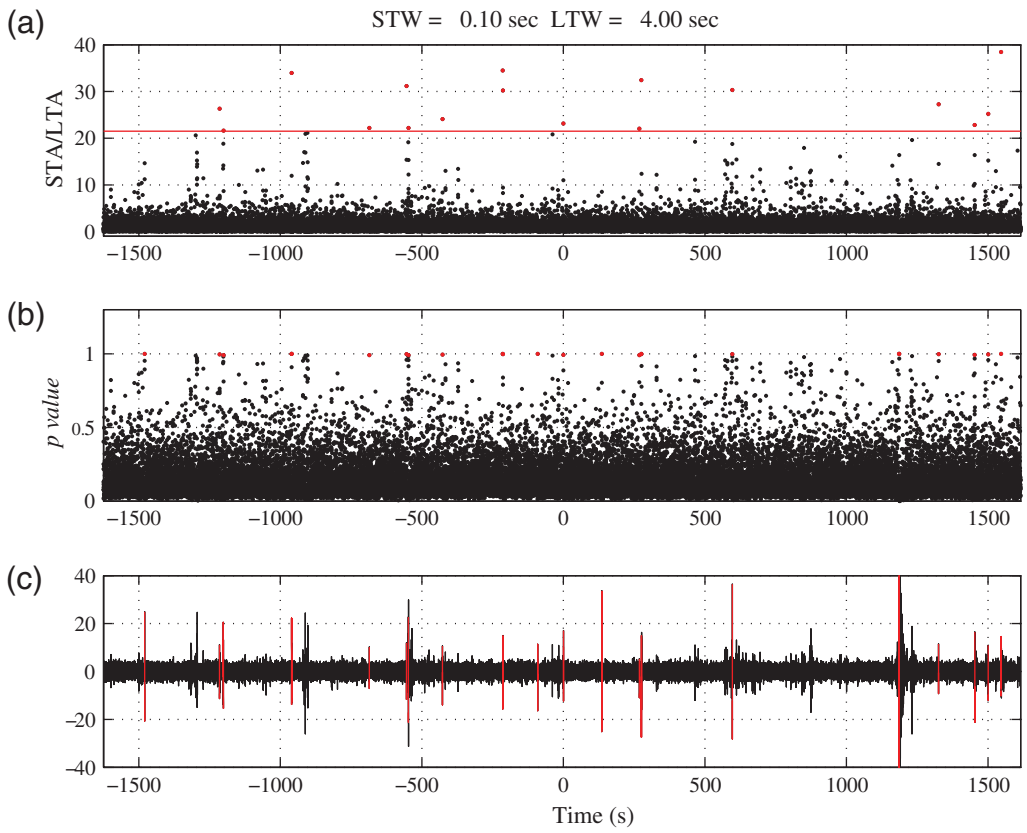

Figure 9. STA/LTA results for a 1 hr time window for the single-channel acoustic signal at LTT03. (a) STA/LTA values (equation 16) for each short-term window shown as dots and critical value for detection shown as horizontal red line. (b) p values given by equation 17 where signal detections are shown as red dots and (c) signal detections on time series shown in red.

To demonstrate this, we apply the spectrogram detector to teleseismic P-wave data from a nuclear explosion. Additionally, for the single-channel acoustic data, there are still a relatively large number of false detections. How would a network of detectors improve performance?

To demonstrate the range of applicability and network performance, we applied the spectrogram detector to teleseismic P waves from a nuclear explosion recorded at the 20-element array at Eskdalemuir, Scotland. EKA is a 20-element array of short-period vertical seismometers arranged in two lines of 10 seismometers with a station spacing of 0.9 km (EKA; e.g., Douglas, 1998). We selected a small (1.7 kt) peaceful nuclear explosion (used for dam construction) from eastern Kazakhstan to analyze data recorded at EKA (epicentral distance of 46.75°) that occurred on 7 December 1974. We selected four (R1, R9, B1, B9) stations at the end of each line so that the noise is uncorrelated between sensors (each line is approximately 9 km long). Figure 10 shows the spectrogram and filtered time series at short-period element R1. In contrast to local recordings, the teleseismic P wave is very band-limited (between approximately 2 and 4 Hz), but is still manifest as a vertical stripe. As before, we selected detection parameters based on a grid search; the signal was detected at each of the four elements with a total of 2 false detections over the four 600 s time segments. In this case, parameters were window length of 1 s, $\alpha = 0.95$, $\beta_1 = 0.5$, and $\rho_1 = 0.1$. Note for the narrow band data, the vertical mask as defined by equation (1) actually degraded the results. We performed a similar analysis for STA/LTA, and detection results were slightly improved. This indicates that at a larger range and/or for narrow band recordings, the spectrogram detector provides no useful gain over traditional STA/LTA techniques.

To demonstrate how a network of spectrogram detectors can reduce false detections, we first note that by the probability integral theorem, the p values for signal detections will in general be uniformly distributed between 0 and 1 under our null hypothesis given by equation (8) (Rohatgi, 1976). We can therefore treat the p values as random variables (RV) drawn from a uniform distribution on the interval [0, 1] (e.g., Bailey and Gribskov, 1998). We then use a data fusion method called Fisher's combined probability test by defining the test statistic

$$X^2 = -2 \sum_{i=1}^{k} \ln p_i. \tag{19}$$

To see this, we use the theorem stating that random variables $X_1, X_2, \ldots, X_n$ with a common distribution function F (in this case uniform) are identically distributed, if and only if

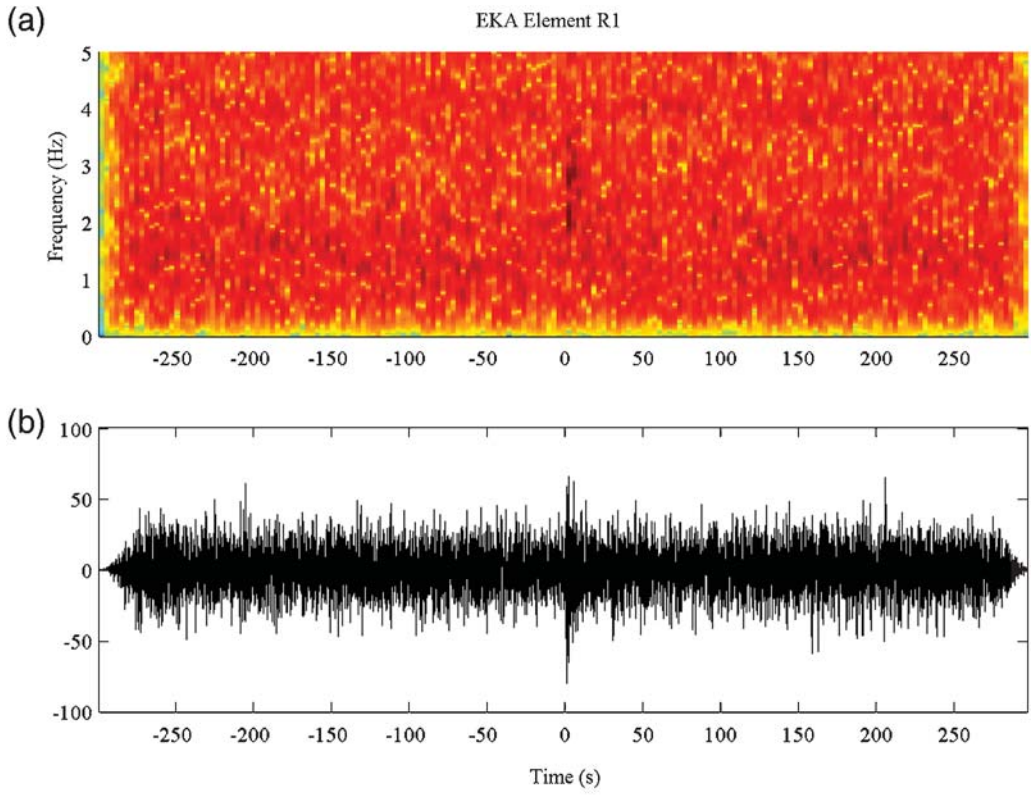

Figure 10. (a) Spectrogram from Kazakh nuclear explosion recorded a short-period element R1 of EKA array in Scotland. (b) Lower portion shows the seismogram band-pass filtered between 2 and 5 Hz.

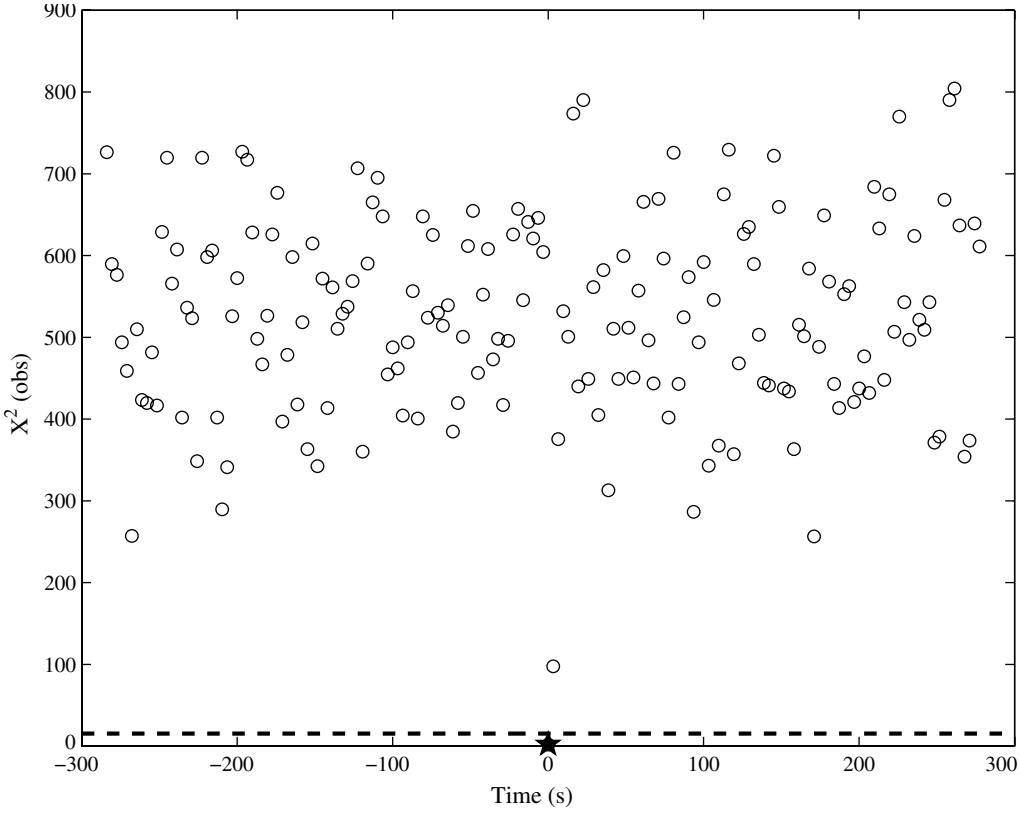

Figure 11. Observed network test statistic, X^2 given by equation (19) for the four EKA stations. Dashed line indicates critical value for $\alpha = 0.99$ and the black star is the value for the signal window.

$$F(x) = 1 - e^{-\lambda x}, \tag{20}$$

for $x \geq 0$ (Rohatgi, 1976). For $\lambda = 2$, this implies that the negative natural logarithm of a uniform RV follows an exponential distribution or equivalently a χ^2 distribution with 2 degrees of freedom. Therefore, the sum of the natural logarithm of p values given by equation (19) is given by a χ^2 distribution with $2k$ degrees of freedom.

We artificially increased the number of false alarms by decreasing β_1 from 0.5 to 0.4 (thereby increasing the number of illuminated bits). This resulted in a total of 20 false detections for the four individual stations. Figure 11 shows the X^2 test statistic given by equation (19) for the spectrogram detector p values using the four EKA stations. The probability of detection is 0.98; there are now no false detections by combining the four stations.

Note that Fisher's method will only work for a limited number of stations where it is assumed that the null hypothesis is true in most cases. For a large number of stations, we could use binomial trials for each cell where a 1 indicates detection and 0 indicates no detection. In this case, a probability of detection could be computed using a technique similar to that previously outlined (e.g., equation 12).

The spectrogram detector described earlier is configured to detect impulsive signal transients and will work best at close ranges. However, we note that different fields of view can be defined depending upon the characteristics of the signals to be detected. For example, volcanic tremor and chugging (e.g., Lees *et al.*, 2004) can be manifest as nearly horizontal stripes on a spectrogram and associated harmonics. Using a horizontal field of view, the spectrogram detector could be used to track the harmonics and their drift as a function of time. We have also used a variation of scan statistics to construct statistically based discriminants from 2D grids of magnitude and distance amplitude correction (Taylor *et al.*, 2002) of Fisk *et al.* (2009). By defining a field of view as a triangle on a 2D P/S plot, we were able to obtain excellent discrimination performance.

Conclusions

A spectrogram detector has been developed that is shown to be effective for the detection of impulsive signal transients (e.g., from small explosions). Impulsive signals are observed as short-duration vertical stripes on time-frequency spectrograms. The spectrograms are transformed into bit-maps after vertical features are enhanced using 2D image-processing techniques. For each time window, a columnwise sum of bits is made over frequency and a probability of detection is computed under the null hypothesis H_0: signal + noise, where it is assumed that the sum can be represented as a Bernoulli random variable. Using 1 hr of single-channel acoustic data containing an arrival from a 1 lb surface explosion recorded at distance of 3.1 km, we show that the spectrogram detector gives better detection performance than a standard STA/LTA detector. We test the range dependence of the spectrogram detector by applying it to teleseismic P waves from a nuclear explosion. Because of the narrow band nature of the signal, the spectrogram detector shows no improvement in performance over STA/LTA. The number of false alarms can be reduced by applying data fusion techniques among multiple sensors using either Fisher's combined probability test or binomial trials. The basic detection technique described in this paper can be adapted to different types of signals depending on their expected time/frequency characteristics.

Data and Resources

The acoustic data used in this study were obtained from experiments conducted by Los Alamos National Laboratory and described in Arrowsmith (2009). Data from the EKA array were kindly provided by John Young of the Blacknest Seismological Centre, UK.

Acknowledgments

Steven Taylor was funded by DOE SBIR Grant No. DE-FG02-07ER84740. Megan Resor provided assistance with spectrogram and STA/LTA computations. Helpful comments from Robert Shumway are appreciated.

References

Allen, R. (1982). Automatic phase pickers: Their present use and future projects, *Bull. Seismol. Soc. Am.* **72,** S225–S442.

Anderson, D. N., and S. R. Taylor (2002). Application of regularized discrimination analysis to regional seismic event identification, *Bull. Seismol. Soc. Am.* **92,** 2391–2399.

Anderson, D. N., D. K. Fagan, M. A. Tinker, G. D. Kraft, and K. D. Hutchenson (2007). A mathematical statistics formulation of the teleseismic explosion identification problem with multiple discriminants, *Bull. Seismol. Soc. Am.* **97,** 1730–1741.

Arrowsmith, S., R. Whitaker, S. R. Taylor, R. Burlacu, B. Stump, M. Hedlin, G. Randall, C. Hayward, and D. ReVelle (2008). Regional monitoring of infrasound events using multiple arrays: Application to Utah and Washington State, *Geophys. J. Int.* **175,** 291–300.

Arrowsmith, S. J. (2009). The use of seismo-acoustics for proliferation detection, *Los Alamos National Laboratory, Los Alamos, New Mexico*, LA-UR-09-07822.

Arrowsmith, S. J., M. D. Arrowsmith, M. A. H. Hedlin, and B. Stump (2006). Discrimination of delay-fired mine blasts in Wyoming using an automatic time-frequency discriminant, *Bull. Seismol. Soc. Am.* **96,** 2368–2382.

Bailey, T. L., and M. Gribskov (1998). Combining evidence using p-values: Application to sequence homology searches, *Bioinformatics* **14,** 48–54.

Blandford, R. R. (1974). An automatic event detector at the Tonto Forest seismic observatory, *Geophys.* **39,** 633–643.

Brown, D. J., R. Whitaker, B. L. N. Kennett, and C. Tarlowski (2008). Automatic infrasonic detection using the Hough transform, *J. Geophys. Res.* **113,** D17105, doi 10.1029/2008JD009822.

Douglas, A. (1998). Making the most of the recordings from short-period seismometer arrays, *Bull. Seismol. Soc. Am.* **88,** 1155–1170.

Dziewonski, A., S. Bloch, and M. Landisman (1969). A technique for the analysis of transient seismic signals, *Bull. Seismol. Soc. Am.* **59,** 427–444.

Fisk, M. D., S. R. Taylor, W. R. Walter, and G. E. Randall (2009). Seismic event discrimination using two-dimensional grids of regional spectral

ratios: Applications to Novaya Zemlya and the Korean Peninsula, *Proc. of the 31st Monitoring Research Review*, Tucson, Arizona.

Friedman, J. (1989). Regularized discriminant analysis, *J. Am. Stat. Assoc.* **84,** 65–175.

Gonzalez, R. C., and R. E. Woods (2002). *Digital Image Processing*, Pearson Prentice Hall, Upper Saddle River, New Jersey, 793 pp.

Gonzalez, R. C., R. E. Woods, and S. L. Eddins (2004). *Digital Image Processing using MATLAB®*, Pearson Prentice Hall, Upper Saddle River, New Jersey, 609 pp.

Guerriero, M., P. Willett, and J. Glaz (2008). Target detection in sensor network using a Zamboni and scan statistics, *IEEE International Conf. on Acoustics, Speech and Signal Processing*, 2425–2428.

Guerriero, M., P. Willett, and J. Glaz (2009). Distributed target detection in sensor networks using scan statistics, *IEEE Trans. on Signal Processing* **57,** 2629–2639.

Hedlin, M. A. H., J. B. Minster, and J. A. Orcutt (1989). The time-frequency characteristics of quarry blasts and calibration explosions recorded in Kazakhstan, USSR, *Geophys. J. Int.* **99,** 109–121.

Hedlin, M. A. H., J. B. Minster, and J. A. Orcutt (1990). An automatic means to discriminate between earthquakes and quarry blasts, *Bull. Seismol. Soc. Am.* **80,** 2143–2160.

Kay, S. M. (1998). *Fundamentals of Statistical Signal Processing: Detection Theory*, Prentice-Hall, Inc., Upper Saddle River, New Jersey, 560 pp.

Lees, J. M., E. I. Gordeev, and M. Ripepe (2004), Explosions and periodic tremor at Karymsky volcano, Kamchatka, Russia, *Geophys. J. Int.* **158,** 1151–1167.

McLachlan, G. J. (1992). *Discriminant Analysis and Statistical Pattern Recognition*, Wiley, New York.

Naiman, D. Q., and C. E. Priebe (2001). Computing scan statistic p values using importance sampling, with applications to genetics and medical image analysis, *J. Comp. and Graphical Stat.* **10,** 296–328.

Niu, R., and P. K. Varshney (2008). Performance analysis of distributed detection in a random sensor field, *IEEE Trans. on Signal Processing* **56,** 339–349.

Oppenheim, A. V., and R. W. Schafer (1989). *Discrete-Time Signal Processing*, Prentice-Hall, Englewood Cliffs, New Jersey, 879 pp.

Otsu, N. (1979). A threshold selection method from gray-level histograms, *IEEE Trans. on Systems, Man and Cybernetics* **9,** 62–66.

Rohatgi, V. K. (1976). *An Introduction to Probability Theory and Mathematical Statistics*, Wiley, New York, 684 pp.

Shumway, R. H., and D. S. Stoffer (2000). *Time Series Analysis and Its Applications*, Springer-Verlag, New York.

Taylor, S. R. (2009). Recommendations for fractional grid count MDAC 2D misfit functions, *Rocky Mountain Geophysics, Los Alamos, New Mexico*, RMG-2009-003.

Taylor, S. R., A. A. Velasco, H. E. Hartse, W. S. Phillips, W. R. Walter, and A. J. Rodgers (2002). Amplitude corrections for regional seismic discriminants, *Pure. App. Geophys.* **159,** 623–650.

Wang, J., and T. L. Teng (1995). Artificial neural network-based seismic detector, *Bull. Seismol. Soc. Am.* **85,** 308–319.

Withers, M., R. Aster, C. Young, J. Beiriger, M. Harris, S. Moore, and J. Trujillo (1998). A comparison of select trigger algorithms for automated global seismic phase and event detection, *Bull. Seismol. Soc. Am.* **88,** 95–106.

Rocky Mountain Geophysics
167 Piedra Loop
Los Alamos, New Mexico 87544
srt-rmg@comcast.net
(S.R.T.)

Los Alamos National Laboratory
P.O. Box 1663, MS D401
Los Alamos, New Mexico 87545
arrows@lanl.gov
(S.J.A.)

Los Alamos National Laboratory
P.O. Box 1663, MS F665
Los Alamos, New Mexico 87545
dand@lanl.gov
(D.N.A.)

Manuscript received 15 January 2010